

Brief Review of Organic Inorganic Hybrid Perovskite Solar Cells (HPSCs)- An Initiative towards Green Energy Sustainability

Jaimin U. Trivedi¹ and Pallavi Ghalsasi^{1,2*}

¹School of Engineering and Technology, Navrachana University, Vasna Bhayli Road, Vadodara- 391 410, Gujarat, India

²School of Science, Navrachana University, Vasna Bhayli Road, Vadodara- 391 410, Gujarat, India

Received: 10 April 2024

Revised: 20 May 2024

Accepted: 1 June 2024

Published: 30 June 2024

*Corresponding Author: pallavig@nuv.ac.in

DOI <https://zenodo.org/records/16668442>

Abstract

The global trend in the automobile and fuel industry has shifted towards the aim for “*green and clean energy*” and shall remain in that domain for the coming decades. Solar Panels are one of the most common yet effective methods. They are found to be installed everywhere ranging from small shops to housing societies to small/large scale industries to the machinery used for outer space like “space satellites” that fly up high in space and sustain for decades by travelling millions and billions of kilometers! Have you wondered; how they travel in space for “millions of kilometers” with limited “fuel” without getting tired/stopped mid-way? Well, the answer to it is “Solar Energy.” Most of the time, they utilize the “Solar power” in space and convert it into an electrical form that not only helps in the satellite movement but also helps run/work other pieces of machinery and tools installed in it that are required for data capture, and analysis. Nowadays, we see lots of “electric vehicles” moving around us. Nowadays, electric charging stations are installed and available everywhere for use. Could you guess how the charging stations get energized? You guessed it right, via “Solar Panels” installed at the roof top. These panels consist of “solar cells” of P and N-type layered materials/substrates composed of organic and inorganic constituents indigenously designed/structured using various solution/coating/fabricative techniques. Using this technique, one can achieve a solar cell of optimal and efficient power conversion capacity while remaining thermally stable at

“pocket-friendly” costs to provide a “*greener,*” “*cleaner*” as well as a “*sustainable*” future to our nature, society, and mankind.

Keywords

Solar Cells (SCs), Hybrid Perovskite Solar Cells (HPSCs), Power Conversion Efficiency (PCE), Tolerance, Octahedral tilts.

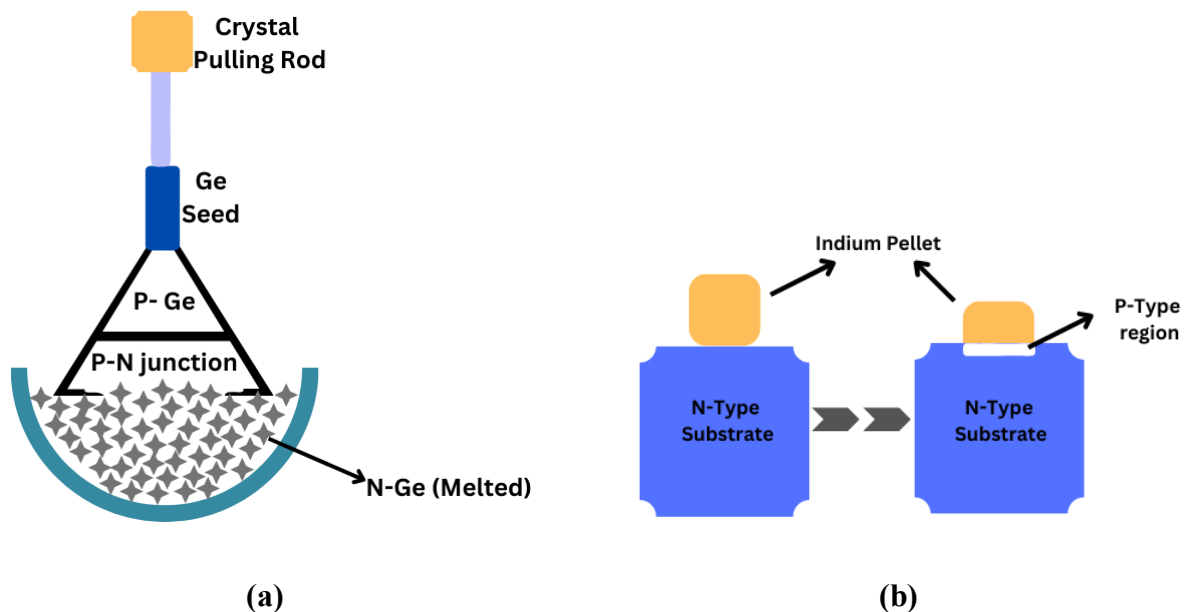
Introduction

What are semi-conductors and P-N junction materials?

The materials that exhibit resistivity between the range of conductors and insulators are termed semiconductors. Silicon (Si), Germanium (Ge), Gallium Arsenide (GaAs) etc.^{1,2} are a few common examples of materials of such types. Ge was the first material to be used in manufacturing electronic devices back in 1939 and 1947, respectively due to its high availability and low manufacturing cost.² But, as it was highly temperature sensitive, it was not used in device fabrications at large-scale. During the 1950's, Si became the prior choice for device construction and fabrication as it was less sensitive to temperature compared to Ge and was available in abundance². Although replacing Ge by Si solved the temperature sensitivity problem in electronic networks, the field of electronics got concerned about the speed issue². As with time, the computers and communication systems operated at faster speeds with high performance, a semiconducting material capable of catering to new needs was required. This resulted in the development of GaAs in the early 1970s². GaAs marked its entry in the field of electronics to overcome high speed issues- i.e., response time required for the fast communications between the devices and networks². To understand the working of these materials, let us dive into their bonding arrangements and understand the underlying mechanism of them. Starting with the bond arrangement of pure Si and Ge crystal- the four valence electrons (i.e. tetravalent) of each atom are shared with their four adjoining atoms to form bonds^{1,2}. Whereas, in case of GaAs, The Ga and As have three and five valence electrons, respectively and so Ga atom bonds with three As atoms while As atom bonds with five Ga atoms. This type of electron shared bonding in the atom is known as covalent bonding^{1,2}. Further, these valence electrons can absorb enough amount of energy by external cause (like temperature) and break the covalent bonding to attain “free state”- A state wherein the electron can move freely inside the material². These free electrons are termed as intrinsic charge carriers and their ability to move inside material is known as carrier mobility. It is important in device

networks as these free electrons can be quickly manipulated for desired functions. As intrinsic charge carriers of GaAs are low, it has the higher carrier mobility of all three materials². Moreover, to improve the characteristics of these intrinsic materials- (i.e. existing in their pure form), the impurity of the level of one part in 10 billion² is added to improve the conductivity of semiconductors.² The process of adding impurities to pure semiconducting materials in a specified amount is known as doping.² Depending on the type of impurities added in to a semiconductor, hole or electron density increases and the respective charge carriers are mobilized inside it¹. By adding pentavalent (i.e., donor) and trivalent (i.e., acceptor) impurities, N and P-Type semiconductors are formed respectively¹. The charge of donor and acceptor ions are positive and negative, respectively. Further, the majority and minority charge carriers in N-type materials are electrons and holes, whereas in p-type materials are holes and electrons, respectively². The p and n-type materials are then combined with external cause- i.e., high temperature heating to form a junction between them. There are three methods that are widely used for p-n junction diode formation. 1). By Grown Junction Method: This is the oldest and most popular method for constructing a diode. It involves use of pure intrinsic semiconductor along with P-type impurity are heated high. They are heated to such an extent where both the matters melt and dissolve in each other. Further, a small semiconducting crystal known as “seed” with required impurity is then placed in the melted solution through the rod/shaft as shown in fig. 1a. Then the rod is pulled out while rotating so that melted solution that has stuck to the seed becomes hard when cooled down. Once the material cools down, it forms a crystal with the same characteristics as that of seed. Furthermore, this larger size crystal is then cut into small sized diode pieces. This is the process of obtaining P-type semiconductor. By adding N and P-type impurities one-by-one, one can form PN junctions, and they can be further cut into small pieces for studying its characteristic properties. As the crystal size is large, it implies that the grown junction region is large and therefore it would be difficult to handle or pass high currents due to high power rating⁵³. Next method is the “Alloy junction method” which is the general one. In this method, a small indium block (of trivalent impurity say) is placed above the N-type material (say Ge slab due to high temp. sensitivity) and heated up to $500^{\circ}\text{C}^{1,2}$. After puddle formation, it is solidified again to normal temperature¹. During the process, the indium block mixture penetrates inside the Ge slab and becomes thick like a button/switch on its outer surface¹ as shown in fig. 1b. Another method is the “Diffusion junction method”. In this method, a thin N or P-type semiconductor is mixed with the impurity present in the gaseous or

vaporized form. Firstly, a thin mask type layer which is open with space in the middle part is put on N-type crystal and then they both are exposed to gaseous or vapor impurity. Then they are heated to a very high temperature in which the vapor impurity enters inside the crystal from the open space of the mask as shown in fig.1c. The impurity gets diffused across the N-type crystal which produces a P-type semiconductor and hence P-N junction is formed. This method provides more control over the accuracy in performing and is widely used; however, it takes more time compared to alloy process⁵³. Hence, the alloy junction method seems to be the simpler and most effective of the three methods. Further, during the junction formation in alloy method, the free electrons and holes in the N and P-type materials diffuse across the junction and combines with each other-i.e., holes from the p-type combines with electrons of the N-region and electrons of N-type combines with the holes of P- region near the junction. This loosens the free electrons and holes of N and P-regions that creates a layer of positive and negative charges near the junction. This is the region of depletion of charge carriers. Hence it is known as depletion region.² The depletion regions stop the further diffusion of electrons and holes and act as a barrier.^{1,2} Due to the positive and negative charges near the depletion region, electric field is produced, and potential developed by it is called barrier potential¹. Due to the barrier potential, the free electrons flow from the N-region across the junction is stopped.^{1,2}



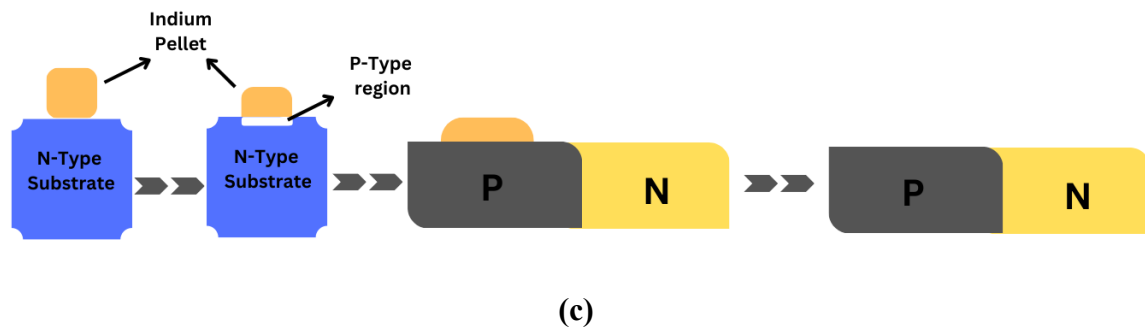


Figure 1: P-N junction formation by (a) Grown Junction Method, (b) Alloy method and (c) Diffusion Junction Method⁵³. The above figures shown are originally inspired from the website (<https://todayscircuits.wordpress.com/2011/06/19/semiconductor-diode-fabrication-types/>). However, the permissions of use/modify have been obtained from the website www.electronicclinic.com.

Note that the movement of free carriers inside the material is random and to unify the flow of current, biasing must be done. “biasing” is providing the external voltage across the junction to get response. It is classified into three biasing conditions- No Bias (Zero bias), Forward bias and Reverse bias conditions, starting with no bias voltage- In this condition, as external bias is zero, no charge movement occurs. Due to the lack of free charge carrier movement, the positive and negative ions remain as they are and therefore no current flows through the depletion layer as shown in fig. 2a. During the forward bias condition, the p and n regions are filled with excess holes and electrons due to which charge carrier movement across p and n junction occurs². The negative terminal produces an excess of electrons in the N-region, and these free electrons combine with positive charge near the junction, thereby making depletion layer smaller (thin). Further, the excess number of free electrons will be able to pass through the junction and combine with holes of p-region and become valence electrons¹. Further, these valence electrons get attracted to the positive side of p-region and move towards the left side of p-region of external bias¹. Similarly, the holes in p-region combine with negative charge near the depletion region, while excess holes get attracted to the right side of n-region of external bias¹. Due to this there is charge carrier movement by the majority carriers, and so the current flows across the junction in the forward direction from p-to the-n-region as shown in fig. 2b. Whereas in the reverse bias condition, the situation is reversed. i.e. The positive terminal of battery is connected to n-region and negative terminal to p-region. Due to this, the electrons and holes get attracted towards the positive and negative terminals of external bias¹, while the minority

carriers absorb lesser amounts of energy. This energy makes them move towards the junction, but it is not enough to cross that. Therefore, they get accumulated near the junction in higher numbers, i.e. higher number of positive and negative charge accumulates, thereby making the depletion layer bigger (thicker) and a very tiny amount current flow occurs from the n-to-p region as shown in fig. 2c. The current flow across the junction in forward and reverse bias is called drift current denoted by I_D . Here, the current flow is done by minority carriers. After a certain time, if we increase the voltage, the current does not increase further. This condition is known as saturation condition² and the current is known as the saturation current denoted by I_S .² The term is common for both forward and reverse current. V-I characteristic curve is shown in fig. 2d. The total current I carried across the p-n junction is given by

$$I = I_e + I_h \quad (1.1)$$

The current equation in general form for biasing conditions is given as

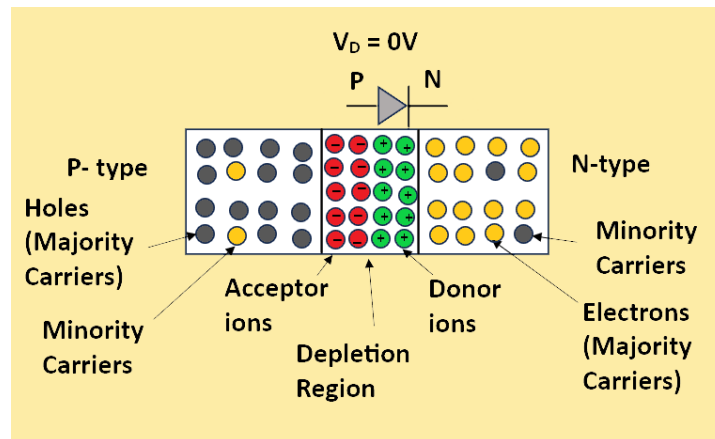
$$I_D = I_S (e^{V_D/nV_T} - 1) \quad (1.2)$$

$$V_T = kT_K/q \quad (1.3)$$

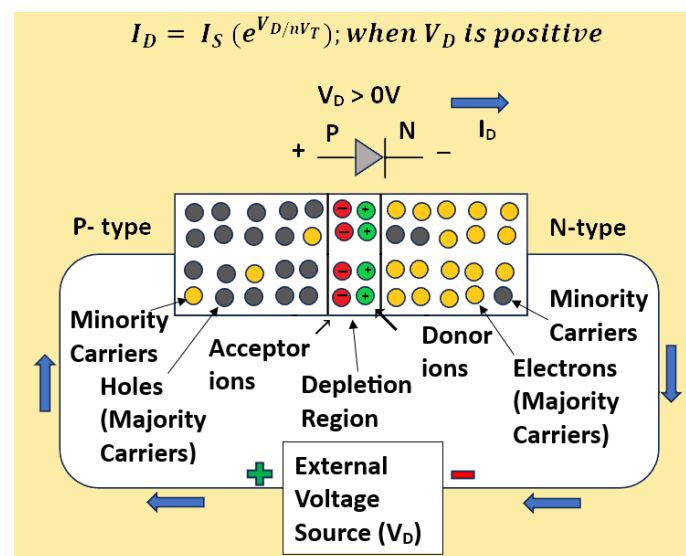
Where V_D , I_S , and n are the drift voltage applied across bias junction, saturation current (in forward and reverse bias) and the ideality factor ($n = 1$). V_T , T_K are the thermal voltage and absolute temperature in Kelvin, k is Boltzmann constant and q electronic charge magnitude (1.6×10^{-19} C).² It can be seen that the drift current increase exponentially with drift voltage during forward biasing while under reverse bias, the drift voltage starts to flow in the “breakdown” region- (region where barrier potential breaks and diode conducts current in reverse direction), The reverse current flows in extremely small quantity (i.e. in micro or nano ampere scale)^{1,2}, hence the exponential term of equation becomes very small and so drift current directly depends on the reverse current as shown in fig. 2d. Hence, the eq. 1.2 is rewritten for forward and reverse bias as follows.

$$I_D = I_S (e^{V_D/nV_T}); \text{when } V_D \text{ is positive} \quad (1.4)$$

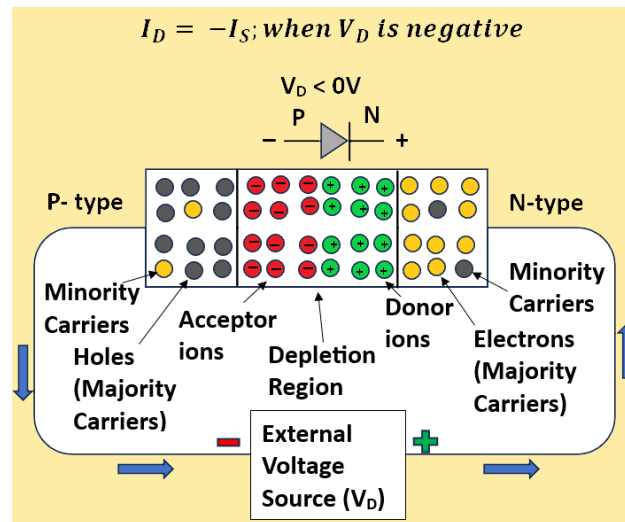
$$I_D = -I_S; \text{when } V_D \text{ is negative} \quad (1.5)$$



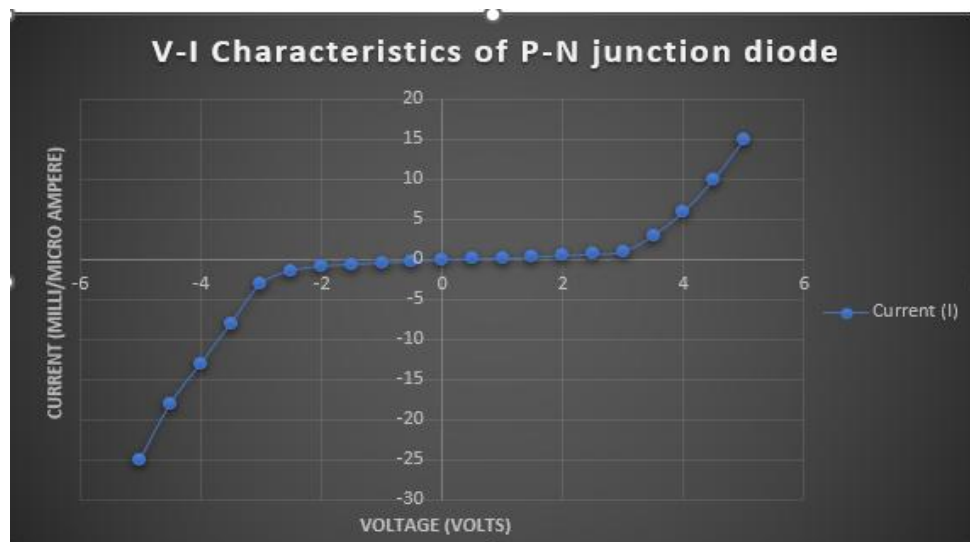
(a)



(b)



(c)



(d)

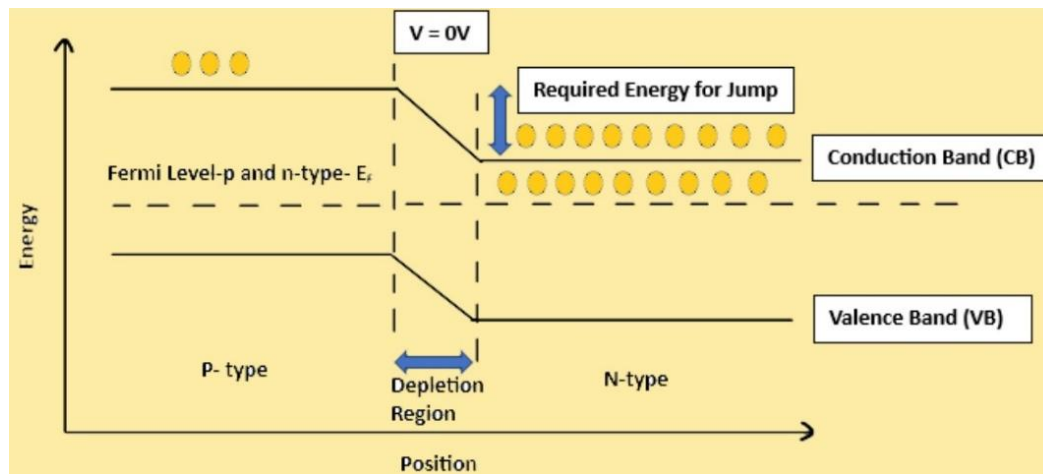
Figure 2 (a-d): Biasing conditions of P-N junction in (a) zero, (b) forward and (c) reverse bias conditions; (d) V-I curve of P-N diode.

Within the individual atom structure, certain energy levels are assigned to each orbital shell having energy range from low-to-high energy state while moving from nucleus to outermost shell² of the particular atom. Therefore, the valence electrons would have a higher amount of energy as compared to the free electrons². When these atoms are brought close together for crystal formation, the electron energies of outer most orbital of the parent atom are slightly differ in energy with respect to the electron energy of the outer most orbital of the adjoining

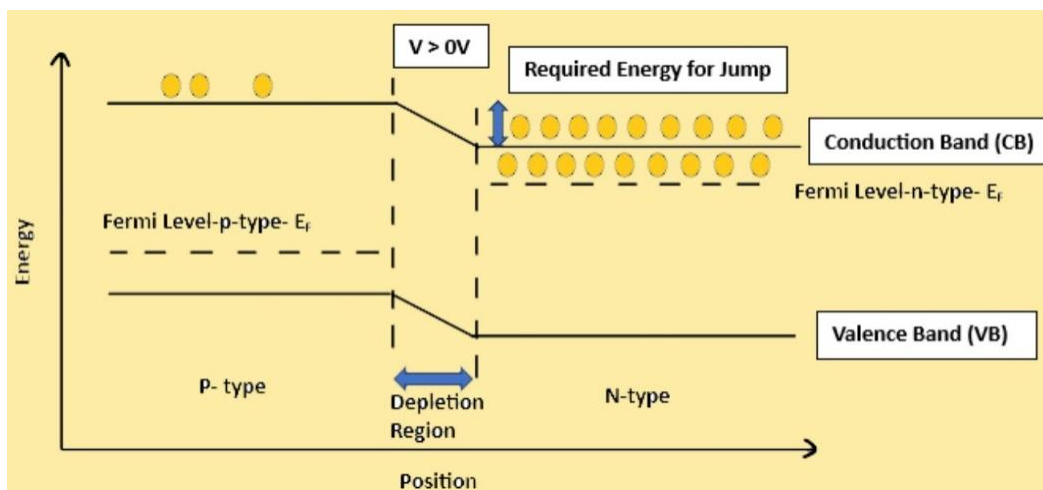
atoms². (i.e. electron energy of orbit of parent Si/Ge atom is slightly higher or lower than that of the Si/Ge atoms sitting adjacent to the parent atom. It is because of Pauli's exclusion principle). Further due to these atomic interactions, the orbital energy levels of valence electrons smear out in the form of bands, resulting in energy band formation-i.e. the Valence Band (VB). Similar is the process for electrons present in the free state. This gives rise to conduction band (CB) formation². Furthermore, due to this energy band formation, there is an invisible/forbidden gap created between the lowermost part of VB and uppermost part of CB. This forbidden energy gap created between the VB and CB is known as band gap². Moreover, the highest energy state that an electron energy can occupy is known as fermi level denoted by E_F .² Moreover, in order to become a free charge carrier, valence electrons require external energy to cross the band gap to reach conduction band. Generally, the energy levels of VB and CB in n-type material are at a lower position than that of energy levels of p-type materials. It is due to trivalent impurity that exhibits lower force of attraction on the outer most shell of electrons, resulting to slightly larger orbits and more energy^{1,2}. During the junction formation, the CB of n and p-regions overlap. It implies that electrons in CB of n-region can diffuse to CB of p-region if they get enough energy (or viz. external bias). It is also important to note that, once the electron crosses the junction and reaches the CB of p-region, it loses energy and rapidly falls on the VB and combines with holes of p-region². Due to this, the depletion layer expands, and energy levels of n-region bands reduce^{2,3}. This will continue until electrons in CB of n-region have lost their energy to cross junction. This condition is known as equilibrium condition². Due to this process, the position of CB and VB of n-region lower down and therefore a "hill" type region gets formed which needs to be crossed by the CB electrons of n-region to reach to CB of p-region so as to generate current flow across the junction. Due to this band lowering, the fermi level of p and n-region coincides with each other as shown in fig. 3a.

In terms of energy band diagram in forward bias, as we know that due to electron-hole recombination at the depletion region, the region becomes smaller (thin). Due to this the CB and VB positions of p-region slightly lower down, and the free electrons that have absorbed sufficient energy can jump from n-region CB to p-region CB and current can flow across the junction as shown in fig. 3b. While in reverse bias conditions, as the minority carriers accumulate near the junction due to insufficient amount of energy, they are unable to cross the junction, hence the width of depletion region gets bigger (thick). Due to this, the position of CB and VB of p-region now lifts up higher. Therefore, the high amount of energy is required

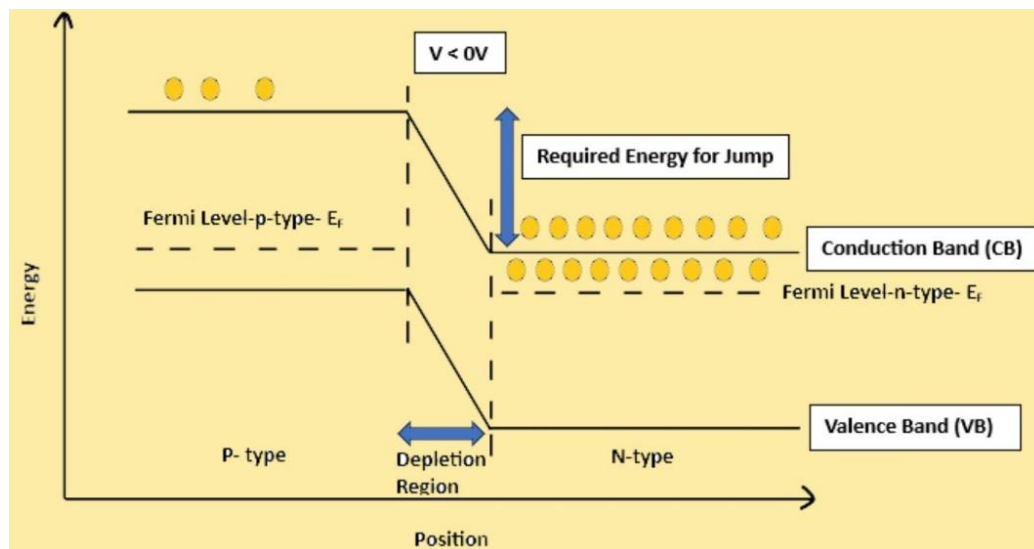
by the electrons sitting in the n-region CB so that they can jump to CB of p-region to generate current across the junction as shown in fig. 3c.



(a)



(b)



(c)

Figure 3(a-c): Energy levels of P-N junction under (a) zero bias, (b) forward and (c) reverse bias conditions.³

What is a Solar cell and how does it Work?

Until now, we saw the working of P-N junction diodes to generate drift current and how their energy bands variate near depletion region under un-biased as well as under three biasing conditions. But can we use p-n junction diode to generate voltage? Well, yes by applying light to this p-n junction diode, we can generate voltage potential across the p and n-region. We know that the p and n-type materials are doped with acceptor and donor impurities, thereby increase the hole and electron density at p and n-regions, respectively. Further, when p and n region combine, the depletion region is formed wherein electron-hole combines with each other and act as a barrier for further electron-hole flow across the junction² (according to fig. 2a). We also know that there is lack of free carriers near the depletion region, the VB must be completely filled while CB must be completely empty. When the light with minimum energy equals to the band gap energy falls on the depletion region, photons will strike the valence band and the electrons in VB will absorb energy and jump to the CB^{2,3}. As electrons jump to CB, they leave holes behind it and electron-hole pairs gets generated inside the depletion region due to the light radiation⁴. Before recombination process starts, these electron-hole pairs get attracted towards positive and negative charges present near the depletion layer, i.e. electrons get attracted by positive charges near the n-region and they move towards the n-region, while

holes get attracted by the negative charges near the p-region and they move towards p-region⁴. This results in charge accumulation of positive and negative charges at both p and n-regions, and a small voltage potential is generated⁴. Further, by applying metal contacts at p and n-sides and connecting it with external circuit a small light bulb can be glowed. Therefore, the light energy was converted to electrical form and voltage was generated without using any external source and hence it is called as “photovoltaic (PV) effect”.⁴ As the p-n junction diode behaved as the cell/small battery that stores charge, which was further used to generate voltage, the p-n junction are also known as solar cells. One important thing to note here is that the activity of the depletion region becomes vital for generating the voltage potential across the p and n-regions as outside the depletion region, the electrons and holes will absorb the light energy and will recombine immediately⁴. Moreover, the solar cell generates direct-current DC. So, multiplying voltage with current will give power. Fig. 4⁶ gives the general I-V characteristics of solar cell.

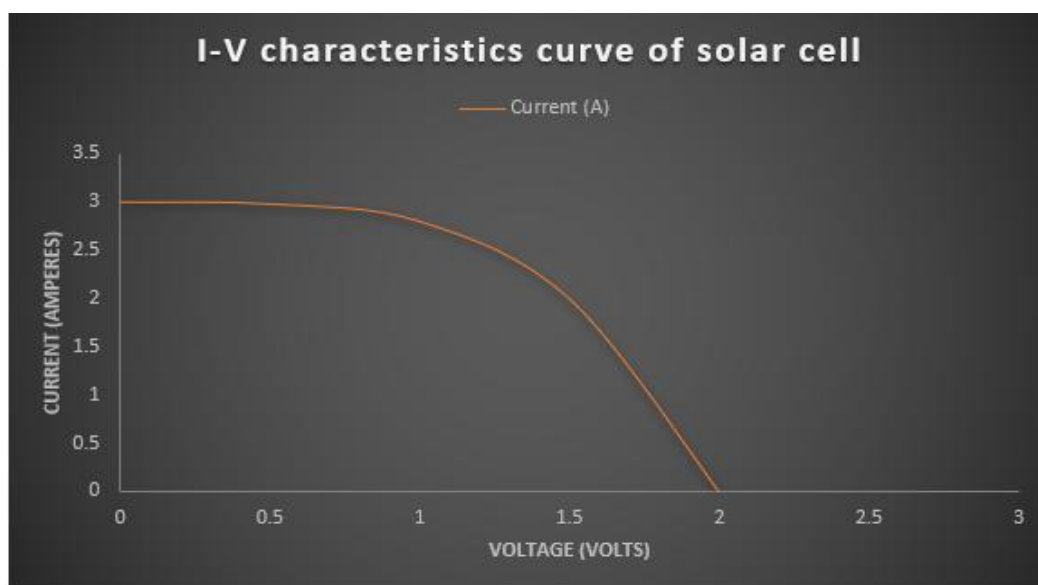


Figure 4: I-V Characteristic curve of the solar cell.

As we know, the solar cell, or PV cell converts light energy into electrical energy^{4,5}. It is a form of photoelectric cell. Solar cell technology started with the discovery of renowned French physicist Antonie-Cesar Becquerel dating back in 1839⁵. He discovered the PV effect and observed voltage developed on the electrode when light falls upon it. Later in 1889, Charles Fritts designed “true solar cell junctions” from a semiconducting coating of selenium Se with a thin gold layer^{4,5}. Although his device conversion efficiency was poor, it converted about 1%

of the total incident energy opening up the doors for semiconducting materials to be used for energy conversion at a cheaper cost. These solar cells were still stuck to a conversion efficiency of 1% until 1954, wherein a breakthrough was achieved by three American researchers. They showed the solar cell efficiency rise from 1% to 6% under direct sunlight^{4,5}. By 1980s, Si cells were further replaced using gallium arsenide GaAs thereby increasing efficiency to 20%.^{4,5}

Let's understand the working of solar cells of single/homo junction. Again, the basic building blocks P-N junction diode, i.e. they mainly consist of P and N-type material layers sandwiched between the junction layer with coated layers and metal grids at top and bottom layer cell surface. Starting with the top layer consisting of N-type Si material. This layer is heavily doped with donor impurity and made deliberately thin (thickness $<1\mu\text{m}$) so that light can easily pass through the layer for PV process.⁵ The top layer is coated with anti-reflective (AR) coating made of oxides of silicon SiO_2 , TiO_2 , etc^{4,5}. The metal contact at the top surface of the cells is the metal finger pattern arranged in the grid form. When the light energy in the form of photon falls on the top layer, electrons in the VB gets excited and jumps to the CB and become free electrons (carriers); i.e. moves from the ground state to excited energy state and reach to the absorber layer⁵. The absorber layer mainly consists of layer of silicon or tin oxides that helps in the electron-hole pair generation to start light-to-energy conversion process. Further, these free electrons that have jumped to higher state leaves hole/vacancy behind it and these electrons get attracted to the donor ions and moves towards the top surface of the cell and pass through the metal grid⁵. Hence, metal grid attains negative charge. Similar process happens with holes, i.e. the holes get attracted towards the back junction layer made of p-type Si. This layer is lightly doped so that holes can pass through them. It is thicker than the top layer (thickness around few 100's μm)⁵. These holes get attracted to the acceptor ions and moves towards the bottom surface of the cell having metal contact layer of Cu or Ag. Hence, they generate positive charge. This generates voltage potential between the top and bottom surface layers of the cell⁵. Now these two potential terminals created at top and bottom surface of the cell behaves as a small photovoltaic cell wherein the light energy has got converted to electrical form. Similar phenomenon of p-n diode is applied over here, i.e. voltage generation occurs due to electron-hole pair generation at the active/absorber layer. When the circuit is short (i.e. closed), the voltage generated is termed as short circuit voltage while when the circuit is kept open, it is termed as open circuit voltage denoted by V_{oc} .⁵ Open circuit voltage plays an important role when it comes to improving device efficiency and performance. Ideally, one solar cell can

generate open circuit voltage V_{OC} of around 0.5V. Fig. 5⁵⁶ depicts the schematic diagram of a single junction solar cell⁵. As discussed earlier, there is immediate recombination of electron-hole pair when light falls on the surface of the p and n-regions. To reduce this recombination loss of carriers at the surface, multi junction solar cells came into picture. The multi-junction solar cells consist of two or more junctions that are introduced near the top and bottom surface of the cell, and they are commonly known as “hetero junction solar cells.”^{5,6} The heterojunction structure offers several advantages. It reduces carrier loss through recombination, leading to more available carriers for cell functioning and improving power conversion efficiency of solar cells. This simpler process also reduces costs⁴, making the heterojunction solar cell a high-efficiency and cost-effective option.^{5,6}

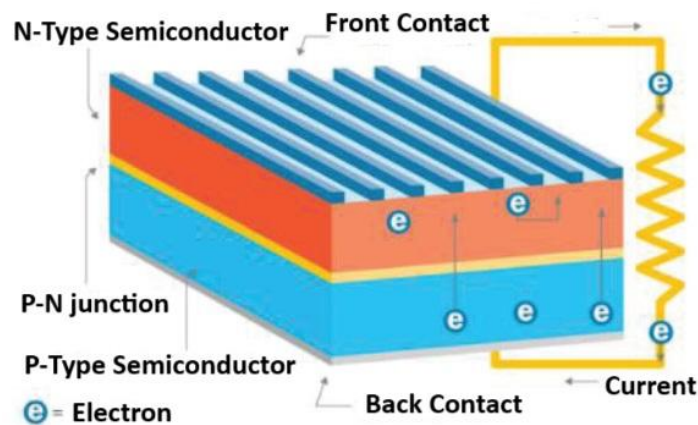
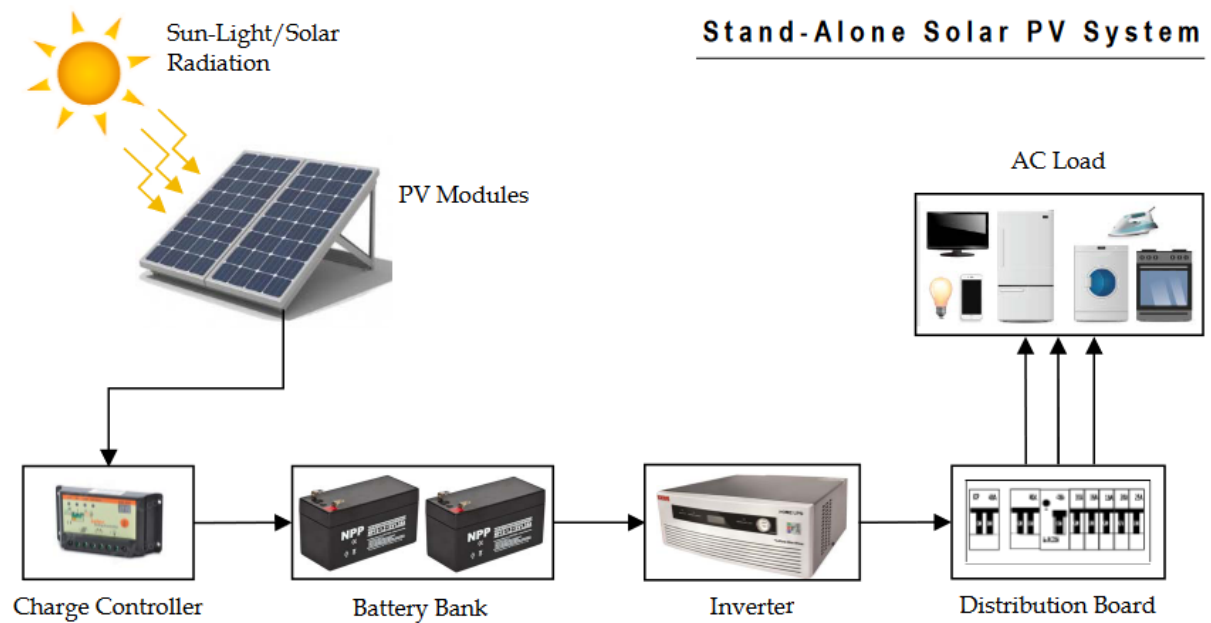


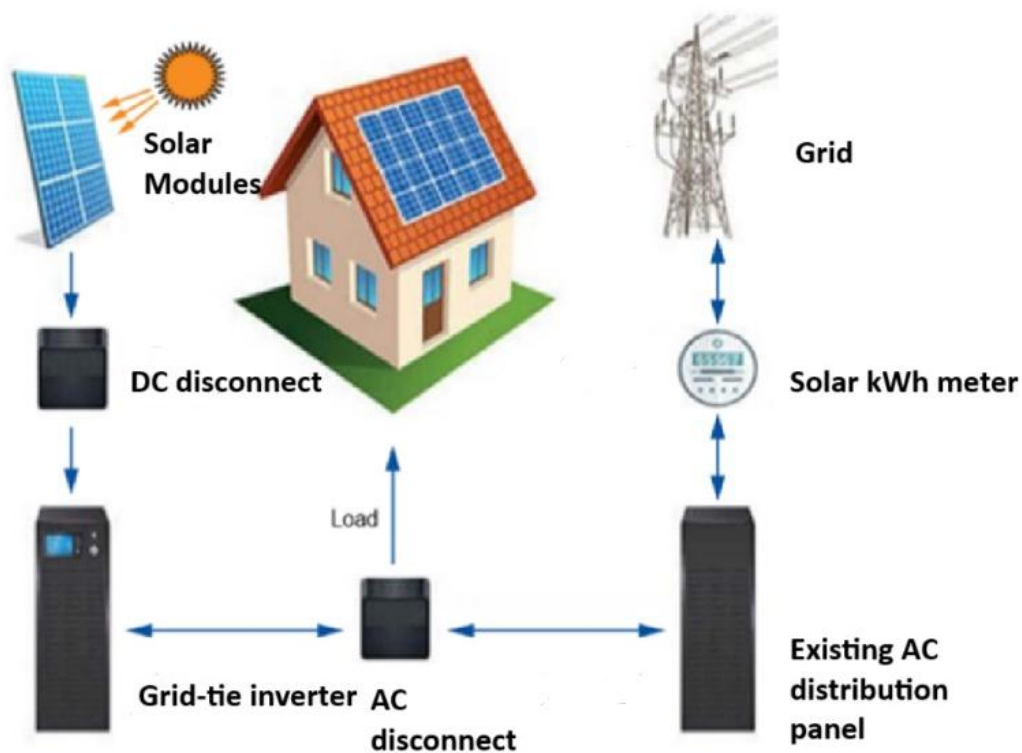
Figure 5: Schematic diagram of a homo-junction solar cell⁵⁶ License: [CC BY 4.0](https://creativecommons.org/licenses/by/4.0/)

Solar Panels: Interestingly, the individual solar cells can be combined to form solar panels for electric power generation from direct sunlight⁴. The arrangement of solar cells can be grouped to form solar arrays consisting of over 1000's of tiny single solar cells to function as solar panels⁵. Each solar cell area size is of few square centimetres (sq. cm) covered by a thin glass coating or transparent plastic coat. For example, a 4" x 4" solar cell can generate a maximum of 2W of power⁵. Depending on the desired voltage or current, the cell arrangement is either in series or parallel configuration, respectively. Combination of group of 36 solar cells constitute photovoltaic (PV) module⁵. This module is interconnected and laminated to the glass of an aluminium frame. Framing and wiring multiple PV modules constitute a solar panel⁵. The back side of the panel contains standardized sockets to combine outputs of all the panels, thereby forming a solar array⁵. To obtain maximum output efficiency from solar panels, two things need to be considered: preferred orientation and angle of the panels. This can be adjusted with

help of latitude degrees of the area location where the panels are installed. Ideally, it needs to be adjusted 15° higher during winter and 15° lower in summer⁵. Reason is that as the sun shines at the front side during the winter and so the panels need to be raised upwards while the sun is at head side during the summer and that's why the panel angle needs to be lowered. In general, one can consider the standard tilt angle of panel with range of plus or minus to the latitude degree of city area to avoid moving panels.^{4,5} Generally, the PV system comprise of four components- Solar panels, a Power system for keeping electric loads, an external circuit and batteries for charge storage. Further, PV systems are of two types- stand-alone and grid-connected⁵. Stand-alone systems contain solar arrays and batteries connected to load circuits to waive off the absence of any electric output coming from the cells at night or during harsh weather conditions⁵. The battery stores charge in the form of direct current (DC) at a constant voltage specified in the panel by their respective companies. The voltage required according to DC and AC load power is fulfilled by DC-to-DC and DC-to-AC converters⁵, respectively as shown in fig. 6a⁵⁷. The stand-alone systems are used in remote areas say for water pumping or to provide power in lighthouses. Another type of PV system is the grid-connected system, i.e., combination of solar array with power grid. Further, this generated power is supplied to the power stations viz. grid network as shown in fig. 6b⁵⁷. The major advantage of this PV systems is that they do not require any battery source to generate power, thereby reducing the component cost however, inverters are required for interfacing low DC volt output stored in the external batteries to be converted to the AC voltage in the grid⁵. Nowadays, the installation of solar panels is found everywhere- in residential places, shops, power stations, industries, etc. They are also used in remote areas where electrical power sources are expensive to install- an initiative towards green energy production⁵.



(a)

On-grid System (solar plus grid import and export)

(b)

Figure 6: (a, b): Stand alone and Grid connected PV cell systems⁵⁷ License: [CC BY 4.0](https://creativecommons.org/licenses/by/4.0/)

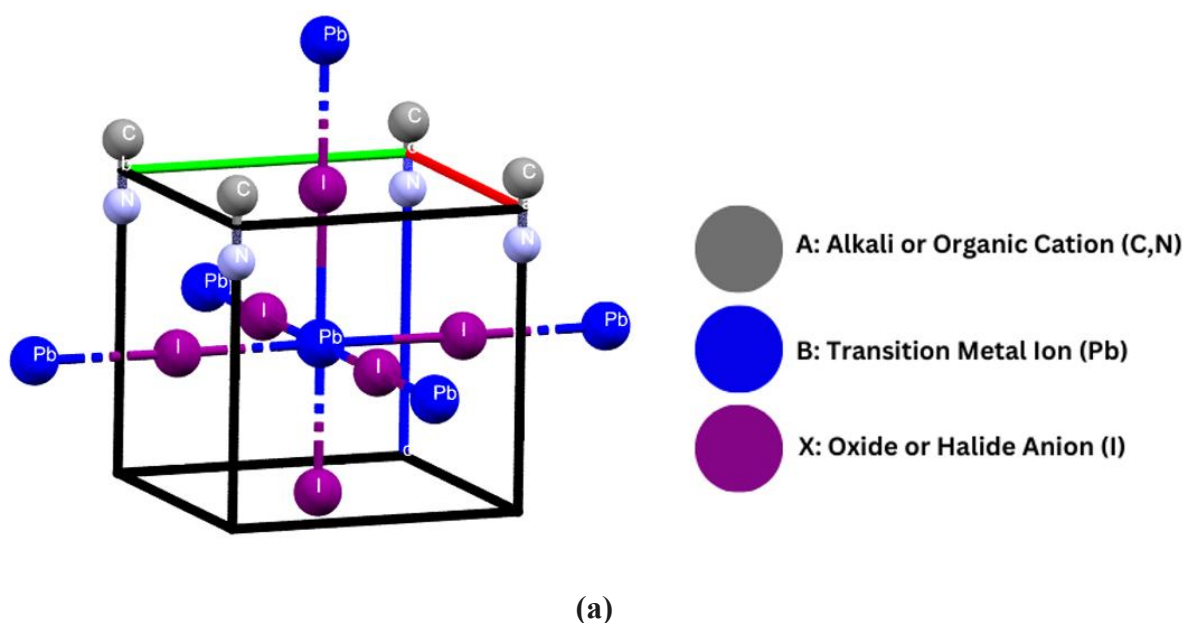
Hybrid Perovskite Solar Cells: What are they and why do we need them?

Hetero/multi-junction solar cells have geared up in the race of “energy sustainability” as lots of research has been carried out and still is the emerging area of research for material Physicists/experimentalists, as they tend to work proactively in this field due to two important reasons as follows (1) Due to the “ease” of cell preparation by spin coating or vacuum deposition technique and (2) Device fabrication by using common materials like Si, Ge, Ti, etc., one can create/design multi-junction solar cells that is stable with optimum conversion efficiency at “cost-effective” rates. It is also important to note that the top, active and bottom(back) layers are now commonly called as Electron transport Layer-ETL, Perovskite Layer and the Hole transport layer-HTL, respectively. These abbreviations will often be used in the discussion from now onwards.

The discovery of the first-ever perovskite material was made in the Russian mountains of Ural back in 1839⁷. The mineral calcium titanate (CaTiO_3) was sent from Saint Petersburg, Berlin by Russian mineralogist August Kammerer to German crystallographer Gustav Rose for further investigation^{11,7}. He found the chemical composition and requested to name the mineral in honour of decorated Napoleonic Wars veteran Count Lev. A. Perovski (1792-1856)⁷.

The general perovskite comprises of ABX_3 formula. Before studying halide-perovskite-based materials these materials were known as “inorganic metal oxides (A= inorganic alkali cation, X= Oxygen anion)¹¹. The basic structure consists of the cubic type having A- cation at the centre site and BX_6 connected internally inside it as octahedral form as shown in the fig. 7a³¹. Fig. 7a is freely available at Cambridge Crystallographic Database (CCDC)³¹. However, metal-oxide-based perovskites are less efficient in terms of light collection capacity. As they have band gaps larger than 2.5 eV, they were not considered good photovoltaic semiconductors¹⁹. To overcome the light absorption efficiency problem, these perovskite materials were substituted with halide anions instead of oxide anions known as inorganic metal halides. These materials provide high light-absorbing capacity with semiconducting properties²⁴. In 2005-2006, A. Kojima et al. researchers started forming various perovskite materials based on this composition. The most common material of study was Methyl Ammonium Lead Iodide (MAPbI_3) which comprised of organic cations instead of inorganic alkali cations²⁶. Also, the replacement of alkali with organic cation proved to be a suitable alternative for light absorbers by replacing organic dyes used in dye-sensitized solar cells (DSSCs)²⁶. This group prepared a

light active layer by solution coating method to improve carrier transport efficiency³¹. They found out that organolead halide perovskite nanocrystals acted as visible light sensitizers on a TiO₂ mesopore film in photoelectrochemical cells. The MAPbI₃ material was deposited with TiO₂ electrode (anode), and Pt glass coated FTO as counter electrode (cathode). The anodic photocurrent got generated under light irradiation at visible wavelength at 800 nm that generated low open circuit voltage V_{OC} ³¹. Due to the low V_{OC} , it showed band gap of around 5.3 eV when Iodine was changed with Bromine²⁶. This showed that organic-inorganic perovskites exhibit different band gaps, thereby achieving power conversion efficiency (PCE) of 3.8% in 2009. This PCE got exceeded to 10% in 2012 when Michael M. Lee and coworkers increased the thickness of perovskite absorber during solidifying the cell structure^{26,31}. The work also suggested improvements to the composition and structure of perovskite materials now commonly known as Hybrid Perovskite materials of organic inorganic type^{26,31}. Generally, the band gap of metal-oxides- i.e. ABO₃ exhibit energy gap from 1.5-2.9 eV, whereas ABX₃ shows wide range of band gap from 1.23-2.5 eV^{26,31}. When the central metal lead gets replaced by tin there is a shift in valence and conduction bands position, due to which the band gap gets reduced from 2.33 (Pb) to 1.96 eV (Sn)³¹.



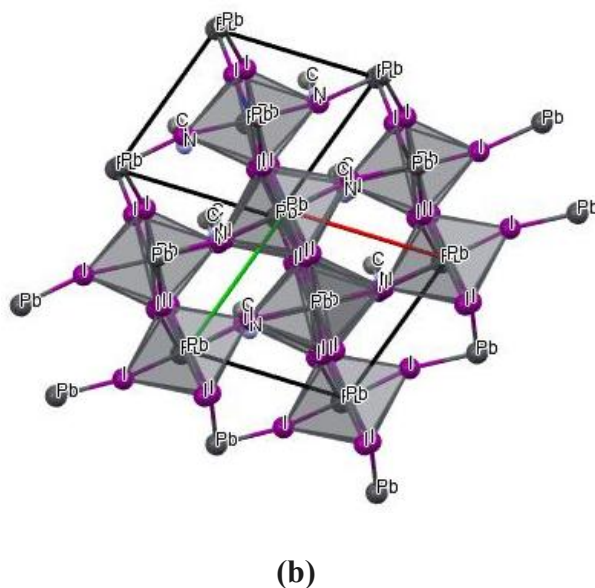


**Figure 7: (a, b) General Unit cell structure of Methylammonium Lead Iodide Crystal-
ABX₃ perovskites CCDC No: 968121, 968125³¹.**

A structural understanding of these perovskite materials is important to analyse the physical properties and stability of these materials³². Fig. 7b shows the crystal structure of methyl ammonium lead iodide with different orientation that is freely available at Cambridge Crystallographic Database (CCDC)³¹. The structure of Methylammonium Lead iodide consists of ABX₃ type wherein A: Organic cation- i.e. Methyl ammonium CH₃NH₃ – sitting at the corners/ edge of the unit cell; B: Central metal- Pb located at the centre surrounded by X: Halide anions in the octahedral form BX₆. The structure of MAPbI₂ exist in the cubic form, whereas MAPbI₃ shows double-storey type structure³¹. However, there is no layered arrangement found. In 2013, three group of researchers discussed about the existence of three different phases of MAPbI₃ crystal; they were cubic (α - phase) (reported by Weber et al)³⁴, tetragonal (β - phase) (reported by Kawamura et al)³⁵ and orthorhombic (γ – phase) (reported by Baikal et al)³⁵. The latter two phases were formed from the former phase. The latter phases are the most common non-cubic PSCs phase studied by the octahedral corner shared network. In terms of tilt angle, β and γ phases have one and all tilt angles other than zero, respectively. In the cubic phase, weber et al. observed large displacement in atomic parameters of MA groups with respect to the C/N and H sites near A-site cations, leading to re-orientation. This rapid reorientation of A-site cations was detected in temperature dependent NMR showing two phase transitions with respect to the low temperature leading to disordering in the structure.

While in the case of orthorhombic phase, the position of A-site cations was fixed and no dynamic movements were observed, leading to structural ordering.³⁵ The work of Baikal et al determined that phases are temperature dependent and reported that α , β , and γ phases occurred at high, room and low temperatures, respectively.³⁵ It highlighted the temperature effect on the hybrid perovskite materials in determining the stability with respect to the rapid reorientation due to C/N and H-site positions^{11,35}.

Using different cations and halides in hybrid perovskite materials like Cs, Rb, etc. along with Methylammonium MA and Formamidinium FA cations with I and Br halide combinations that helps in improving stability and device performance.³⁶ Due to the large displacement in atomic positions of A-site cations, there is reorientation that leads to the tilting effect in the octahedra due to H bonding. As a result, it leads to shrinking of lattice structure.³⁵ Partially replacing MA/FA PbI_3 with Cs, Rb helps the material to get thermally stable and conversion efficient³⁶. Recently, Rb-doped CsFAPbI_3 reported PCE of around 20.3% that were used to fabricate highly durable PSCs that work for over 1000 hours under sunlight^{36,37}.

The structure evolved for PSCs are described below. It mainly exists in three forms: (a) mesoscopic structure (n-i-p), (b) planar structure (n-i-p) and (c) planar inverted structure (p-i-n) as shown in Fig. 8⁵⁸. The (a) is the first and original design of perovskite photovoltaic material used in fabricating high performance devices. Device configuration for (a) is Glass/FTO (Fluorine-F doped Sn oxide)/c-TiO₂/mesopore (mp)- TiO₂ (ETL)/active layer/HTL/metal electrode^{11,12}. In device fabrication, it starts from ETL layer which is the top layer deposition followed by mesopore mp-TiO₂ or mp-Al₂O₃ film on FTO layer coated with glass substrate. Further, the perovskite active layer- i.e., the absorber layer is deposited over ETL layer by annealing method^{11,12}. After annealing, the thin HTL layer- i.e., bottom layer is deposited onto the active layer of perovskite and metal electrode. This completes the device fabrication process in (a)¹². Similar type of fabrication process is carried out in (b). The only difference is that (b) structure is without mp-TiO₂ layer. People found out that mp-TiO₂ layer is not essential for PCE and so another form of planar structure using organic solar cells was derived that was named as inverted planar structure (c)¹². This configuration opened the doors of wide range exploration of various hybrid materials for charge carrier layer. (c) structure configuration is: FTO/HTL/Perovskite active layer/ETL/Metal electrode¹². PSCs results showed that PCE depends on the type of ETL and HTL materials chosen for fabrication

process, because they help in reducing carrier recombination^{11,17}. Moreover, the ideal thickness of the ETL- top layer $<1\mu\text{m}$ while the thickness of HTL- bottom layer lies in the range of few 100's μm . The thickness range of perovskite absorber and contact layers lies within the range of few 160-900 nm.⁵² The fluorine doped tin oxide layer (FTO)- contact layer has the thickness of around 450nm.⁵⁴ The thickness of the layer is related to the carrier diffusion length. The higher the diffusion length, longer will be the time it will take to recombine with charge carriers. Hence, the lower the carrier recombination efficiency, the higher the PCE of the layer will be. Furthermore, it was found that by replacing the contact layers of FTO with ZnO configuration, the thickness was reduced from 450nm to between 300-400nm⁵⁴, well below $1\mu\text{m}$. The lower the thickness, the higher will be the diffusion length and higher will be the power conversion efficiency. Thus, it is observed from the earlier literature carried out by researchers that the selection of contact layers plays a vital role in determining efficiency.

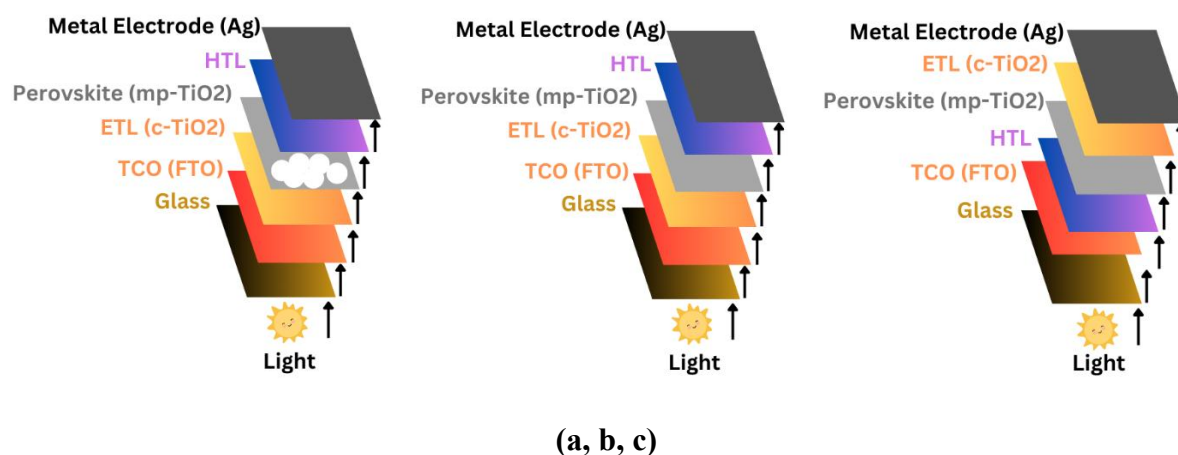


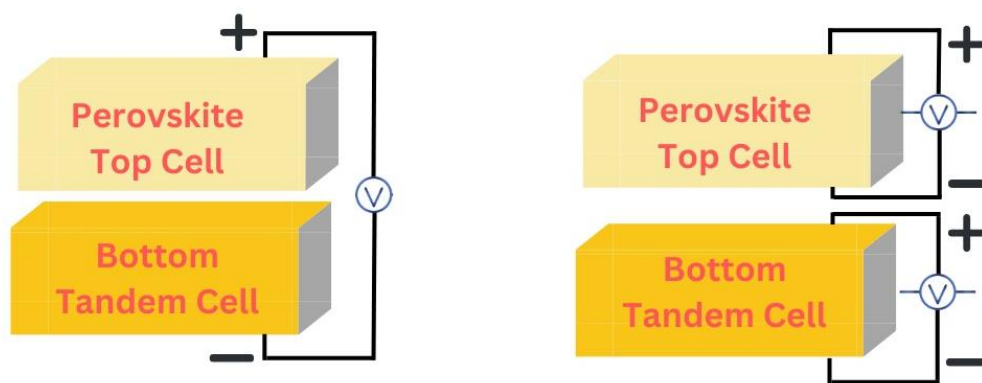
Figure 8 (a-c): Structural Improvements of PSCs; (a) mesoscopic structure (n-i-p), (b) planar structure (n-i-p) and (c) inverted planar structure (p-i-n).⁵⁸ License: [CC BY 4.0](https://creativecommons.org/licenses/by/4.0/)

Up till now, the hybrid perovskite materials mainly consisted of lead Pb as the central metal ion are discussed. However, the fact that Pb is a toxic material when it comes to environment safety. This has been a point of concern and one of the biggest quests is to get the “best alternative”¹² to Pb that can maintain device stability but also give optimum conversion efficiency at the same time to researchers and scientists since late 1980s. The Lead is highly toxic to living organisms and it primarily results from human activity. While lead halide perovskite solar cells (PSCs) offer higher efficiency, they possess potential toxicity. Widespread adoption of PSCs could result in dangerous lead leakage into the environment, posing a significant threat.⁵⁵ It is important to implement solid management and preventive

measures for the safe utilization of PSCs, which includes the development of lead-free alternatives Sn has been one of the most promising candidates in this quest. As discussed earlier, the band gap reduction was observed when the Pb based perovskite material was replaced by Sn¹². There are certain tin Sn-based metal halide materials comprised of MA and FA cations- i.e. MASnI₃ and FASnI₃^{39,41}. They exhibit higher efficiency and are useful for photovoltaic applications. Further, the Sn-based halide systems are the best and most effective alternatives in photovoltaic semiconductors when treated under oxygen-free environment⁴¹. To overcome this, the reducing agents were inserted into the structural device to enhance the oxygen stability⁴¹. The film technique is common for all types, consisting of lead/tin-free inorganic metal halides. As discussed earlier, the organic-free compositions for photovoltaic absorbers, such as Cs-based lead perovskites, has been studied extensively to provide thermal stability with increased efficiency³⁶. The CsPbI₃ PSCs have shown increased efficiency from 2.9% to 18.4% with moderate band gap accounting for phase stabilization^{36,42}. Whereas, the Br-mixed CsPbI₃ and CsPbI₂ materials showed a bandgap of 1.9 eV, with a high-efficiency photovoltaic effect^{36,42}. Although, it produced a slightly lower PCE of 15.5%, but with enhanced open circuit voltage Voc up to 1.43 V, the highest Voc obtained with visible-light harvesting PSCs⁴² so far. Furthermore, it was found that replacing Pb with silver/bismuth-Ag/Bi absorbers showed higher capacity of PCE (>10%) under poor lighting conditions⁴³. This work indicated the potential of PSCs applications of these lead-free devices in the field of information technology-IoT⁴³. Moreover, the work on antimony (Sb) based halide perovskites have also displayed good photovoltaic response along with its conversion efficiency similar to that of Bi absorbers⁴⁴. Cesium antimony-based halide material – Cs₃Sb₂I₉ reported high light absorption with an energy bandgap of 2.05 eV⁴⁵. Seok and coworkers synthesized a chalcogenide-halide mixed perovskite, which demonstrated the best PCE of 3.08% with an optical gap of 1.3–1.4 eV⁴⁷. Other interesting lead-free compositions studied by researchers include titanium-Ti-based halide perovskites showed bandgaps E_g of ~1.38 eV. Sn, Sb, Ag/Bi, and Ti-based hybrid perovskite materials seem to be the potential and reliable candidates for showing good photovoltaic semiconducting properties in terms of visible light absorption³⁶, providing thermal stability³⁹ as well as achieving PCE^{45,46}. One of the important benefits of HPSCs is Voc which is dependent on defects formation in the bulk layer at the interface⁴². As seen above, E_g < 1.6 eV implies Voc is higher along with minimal defects in the interface⁴².

Dye-sensitized solar cells (DSSCs) have emerged as one of the important PV technologies when it comes to device fabrication in solar cells⁴⁸. It was developed by Professor Grätzel in 1991 keeping in mind about environmental safety⁴⁷. However, due to low conversion efficiency, it took time to gain attention similar to thin film technology. But, despite low attention, many researchers worked on this area and extracted organic dyes from natural materials like flower calyx, root, stem bark, leaf etc⁶⁸. that is inexpensive when compared with thin film constituents and analyzed to determine their potential capability of having light absorption properties thereby giving good PCE⁴⁸. Currently, around 13% PCE is achieved by this organic dye extraction in DSSCs technology, and it is believed to cross 15% by the time of the commercialization period^{48,49}.

As discussed earlier about the solar panels operation, it is important to design and fabricate hybrid solar cells aiming towards large scale production and commercialization in all the possible energy sectors. One such approach is done by Tandem solar cells technology- i.e. Si-Tandem solar cells⁵⁰. As aware, Si is abundantly available on earth and so it can be used in design and fabrication of multi junction solar cells with affordable making cost. The working of tandem solar cells is similar to that of a homojunction solar cell as discussed earlier. i.e. light falls on the metal grid and AR coated surface at the top N-type Si layer. This light energy gets converted into electrical form and a small voltage potential is generated by the solar cell. Further, when the light falls on the grid, metal blocks the light and due to it there's a large energy loss^{50,53}. To overcome this problem, two or more solar cells are combined and structured such that, the light falls on the top cell first. This top cell consists of perovskite absorber layer due to which it absorbs the maximum light, and a very few amounts of photon energy reach the bottom cell. The bottom cell consists of Si layer This helps in reducing thermal loss as most of the energy is absorbed by the top cell. This can be understood from the fig. below; (a) Monolithic (2T) Tandem solar cells¹⁷ (as shown in Fig. 9a and 9b³²). However, individual connections are required to be given to the additional contact layers for the bottom contact of the top cell surface and top contact of the bottom cell surface¹⁷. The layers can be of transparent conducting oxides (TCO)⁵⁰.



(a, b)

Figure 9: (a, b) Schematic diagram of Si-Tandem solar cells of two and four terminal (2T and 4T) systems³² License: [CC BY 4.0](https://creativecommons.org/licenses/by/4.0/)

Tandem solar cells consisting of multi-junctions are likely to achieve over 30% efficiency within a few years which shall lead PSCs materials towards large-scale productions⁵⁰.

Where there are benefits of hybrid PSCs, there are certain challenges that need to be overcome for their large-scale application and commercialization⁵². In order to do that, several methods are available by which it can be done; blade coating: the method used for thin film deposition at larger areas; slot-die coating: the roll-to-roll print of flexible PSCs to attain good PCE⁵², etc. Here, first and the foremost concern in it is the “Large area fabrication of solar cells^{5,41,52}”. We know that the structure of hybrid PSCs plays a crucial role in determining stability and maintaining good PCE balance. In the real world, the solar cells are treated under extreme conditions like high humidity, temperature, and extreme solar illumination under severe weather conditions⁵². In these areas, PSCs tend to lack as they show shorter carrier lifetimes due to layer instability in perovskites when exposed to extreme environments. Due to this, maintaining good PCE in a large area is very challenging⁵².

The stability and conversion efficiency of organic-inorganic hybrid perovskite solar cells depends on several parameters such as tolerance limit, carrier diffusion length, Energy gaps, etc. These parameters help tweak/tune the physical, light and electronic properties.

Tolerance factor: The tolerance factor (t) is a vital parameter used to express the stability of perovskite compounds¹¹ and is calculated using the Goldschmidt’s⁸ equation as;

$$t = (r_A + r_X) / \sqrt{2(r_B + r_X)} \quad (1.6)$$

Wherein r_A, r_B, r_X , are the ionic radii of A, B and X-site atoms as shown in Fig.10. It is important for designing hybrid perovskite materials as it plays a crucial role in interpreting perovskite stability and device performance¹¹. However, this equation is not enough for identifying stable perovskite-based halide materials especially iodide based as it showed only 33% tolerance accuracy. To overcome this, Scheffler and co-workers introduced a new factor in 2019^{9,40}. Hence, the new equation is given by

$$t = \frac{r_X}{r_B} - n_A \left(n_A - \frac{r_A/r_B}{\ln \frac{(r_A)}{(r_B)}} \right) \quad (1.7)$$

Where n_A is the oxidation state of A site atoms. Apart from tolerance, the octahedral tilt factor μ ¹⁴, is calculated as the ratio of radii of B and X-site atoms as follows.

$$\mu = r_B/r_X \quad (1.8)$$

This is crucial for understanding the structural stability of perovskites. The t and μ values of mixed-cation perovskites can be calculated by considering the effective radius of A and X-site atoms. Generally, materials with $t = 0.8-1.0$ ^{10,13} are considered to adopt a perovskite structure, while non-perovskite phases form at $t < 0.8$ and $t > 1.0$. It indicates a rather narrow region ($t = 0.91-0.98$)¹⁸ for the formation of the single perovskite phase. Further, Mixed-cation hybrid perovskites are important for solar cell fabrication^{10,16,18}. The t value guides the design of multi-cation perovskites. Guidelines are given for different alloys¹¹. The selection of an ideal t can be achieved through the mixing of A-site cations. The r_A value governs the t value of the alloys. The incorporation of smaller MA⁺ moves towards the favourable value, generating a stable cubic perovskite phase. FAMAPb (I, Br)₃ absorbers are often made near the border of $t = 0.98$ ^{20,40}. The Cs⁺ incorporation plays a key role in forming structurally stable perovskites, thereby reducing $t = 0.85$. Therefore, a small amount of Cs⁺ (doping) leads to the improvement in forming a suitable perovskite crystal¹¹.

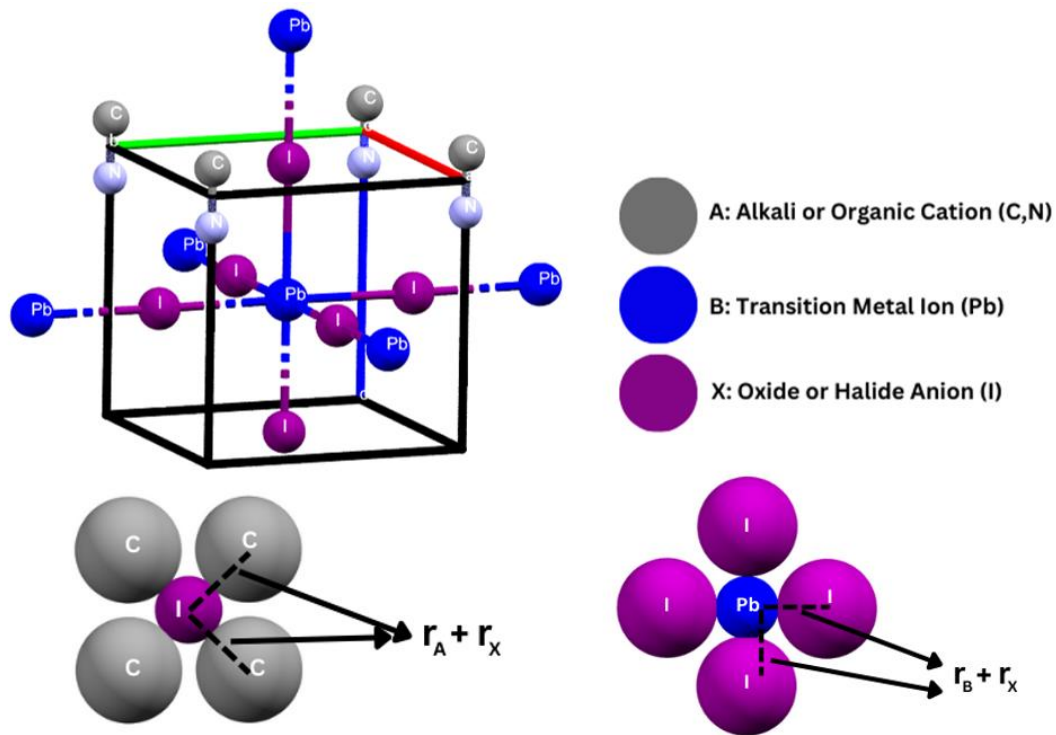


Figure 10: Calculation of Goldschmidt's factor (t) for perovskite structure CCDC No: 968125³¹.

Carrier transport properties: The transport of photo-generated carriers is crucial for the operation of photovoltaic devices^{21,23}. The average length of charge carrier movement between generation and recombination region is known as carrier diffusion length. In solar cells²¹, the carrier *diffusion length* (L_D) is a key parameter^{22,25,28}; determined by carrier mobility (μ^*) and lifetime (τ). Hybrid perovskites, like MAPbI₃ and FAPbI₃, exhibit high (μ^* , τ) resulting in large L_D due to the absence of deep defects^{21,23}. The carrier lifetime for MAPbI₃ single crystals varies between 8 - 175 μm and for thin films, it varies between 0.1 - 23 μm ²⁵. The carrier transport characteristics of MAPbI₃ thin films contribute to the high efficiency of solar cells using MAPbI₃ as a light absorber²⁸. The work of Bi.Y. et al also discussed various hybrid perovskite materials used in solar cells, their properties, crystallinity, and the effects of different cations and anions, as well as the relationship between carrier scattering and various parameters^{25,28}.

$$L_D = \sqrt{D \cdot \tau} \quad (1.9)$$

$$D = \left(\frac{k_B \cdot T}{q} \right) \cdot \mu \quad (2.0)$$

In terms of light absorbing efficiency, the choice of A, B, and X-site species in perovskites and the variation of cations and anions lead to a large variation in light absorption characteristics^{11,27}. Moreover, the light-matter interaction is described by two physical quantities; the refractive index (n) related to electromagnetic wavelength of radiation and the extinction coefficient (k) related to magnitude to electromagnetic wave¹⁵ as shown in the equation below.

$$N = n - ik \quad (2.1)$$

Where N is the single complex number of refractive indices. Further, the stability is also dependent on the variation in the energy gap (E_g) of hybrid perovskites²⁹, which varies with measurements and analysis methods. This variation will influence the E_g values of A-site cation and X-site anions, thereby impacting the alloying as well as the band energy alignment of valence band maximum (VBM) and conduction band minimum (CBM)^{29,30}.

Solar Cells-Types	Materials Type	Bandgap range (eV)	Tolerance factor (t)	Open Circuit Voltage (V_{oc})	Power Conversion Efficiency (PCE) (%)	Limitations/Challenges faced by Solar Cells
Homo-junction (ABO_3)	Metals (Ca, Bi, Pb) + Oxides	1.5-2.9	>1.0	Low (<1V)	Lower (<1%)	Low light absorption capacity due to large bandgap, resulting to lower PCE
Homo-junction (ABX_3)	Metals + Inorganic metal Halides (Br, I)	1.23-2.5	>1.0	Low (<1V)	Lower (1-6%)	Moderate light absorption capacity with slightly lower band gap. But overall lower PCE
Hetero junction ($MAPbI_3$)	Organic cation + Inorganic	1.2-1.9	Between 0.9-0.98	Between 1-2.5V	High (12% to 30%)	Intense light absorption capacity with semiconductor like band gap value, resulting in

	metal + halides					significantly higher PCE compared to other solar cells.
Hetero junction (Cs, Rb doped MAPbI ₃)	Organic-Inorganic metal + halides + (dopant metal like Cs, Rb)	Between 1.1-1.6	Between 0.8-0.9	Between 1-2.5	High (12% to 16.1%)	Intense light absorption capacity with good band gap range. Although slightly lower PCE than PSCs but with significant tolerance and V _{OC} limits.

Table 1: Representation of the comparison of Solar cells with solar and optical parameters.

Shockley-Queisser (SQ) Limit: The Shockley-Queisser (SQ) theory provides a straightforward method to calculate solar cell parameters based on the band gap (E_g) of a semiconductor light absorber³⁸. Importantly, it should be noted that the SQ limit tends to overestimate the solar cell efficiency limit as it relies on simple assumptions³⁸.

Although, PSCs have reached the efficiency mark of 30% but it is also important to note that to achieve higher PCE several factors like tolerance limit, carrier transport properties, layer thickness, etc. needs to be considered to reproduce a solar cell/module that is viable for large scale area production and commercialization purpose. Here, the hybrid PSCs act as “saviour”. The freedom to adjust the layer thickness of desired value in organic and inorganic part, one can tweak/tune the band-gap and achieve a solar cell of optimum efficiency along with tolerance factor lying in the region 0.8-1.0.^{10,33} As we know the correlation between thickness and efficiency⁵⁴, this work will be helpful to the researchers working in this field that can design and modify the cell structures, thickness, etc. which will provide a solar module/device with optimum stability, significant PCE value at the lower costs.

Recent Advancements/Progress carried out in Hybrid Perovskite Solar Cells (HPSCs):

Research-based on HPSCs photovoltaics involves applications in various fields ranging from domestic to industrial scale. The process includes synthesizing materials using a solution-based

chemical process, characterizing perovskite semiconductors using physical methods, and fabricating devices using chemistry, physics, and electronics^{17,52}. Progress in enhanced efficiency and stability depends on the development of new materials and the fostering of the connection between different disciplines. These materials can have a high tolerance factor^{9,37} leading to a larger lifetime for photoexcited-free carriers required for achieving higher PCE^{10,13}. This is especially useful for indoor power sources in IoT⁴³ applications, where high voltage is required to power devices and their secondary batteries under weak light. The goal of perovskite photovoltaics is to mimic the excellent photophysical properties of perovskite-halide materials having an open-circuit voltage and power conversion efficiency close to the Shockley-Queisser limits^{38,41}. Perovskite modules are expected to practically achieve more than ~22% efficiency, making them suitable for commercial devices in terms of cost performance⁵⁰. Additionally, research and development efforts are focused on enhancing the stability and durability of the modules and finding environmentally safe alternatives to lead, such as Sn, Bi, Sb, and Ag³⁶⁻⁴⁴. The field of perovskite science and engineering is anticipated to achieve notable progress in various applications, such as LED, photodetectors, and lasers, apart from photovoltaics¹⁷. Recently in 2020, New Energy and Industrial Technology Development Organization (NEDO) and Panasonic Corporation achieved an extraordinary PCE of 16.1% with hybrid PSCs thin film technology that opened up the potential capabilities and large-scale possibilities for industrial commercialization.^{11,17,52} Therefore, looking at the potential capability of organic-inorganic HPSCs, the future of green and clean energy seems to be lying under their hood in the coming decades, wherein green energy shall be the need of an hour not just for running home/shop appliances, but it shall take up the place in the large scale manufacturing and production based industries to overcome the power consumption and fuel cost. Although the movement is in small steps, the steps taken in this field are guiding us towards the sustainability of green energy that shall assure the sustainability of humanity and the environment.

Acknowledgements

The author thanks his colleague Mr. Sunil Vankar for providing valuable inputs to the discussion.

The author also thanks the following organizations for providing the financial assistance; (i) Scheme of Developing High Quality Research (SHODH), by Knowledge Consortium of

Gujarat (KCG), Gandhinagar, Gujarat & (ii) Navrachana University, Bhayli, Vadodara, Gujarat for providing the fellowships to carry out research work.

References

1. Mehta, V.K. & Mehta, R. (2008). *Principles of Electronics* (11th ed.). India: S. Chand & Company Ltd.
2. Boylestad, R. L. & Nashelsky L. (2014). *Electronic Devices and Circuit Theory* (11th ed.). USA: Pearson New International Edition.
3. Kittel, C. (2005). *Introduction to Solid State Physics* (8th ed.). USA: John Wiley & Sons, Inc.
4. Stand Alone PV System for Off-grid PV Solar Power. (2024). Alternative Energy Tutorials. <https://www.alternative-energy-tutorials.com/solar-power/stand-alone-pv-system.html>
5. Fonash, R. T., & Ashok, S. (2024). solar cell | Definition, Working Principle, & Development. In *Encyclopedia Britannica*.
<https://www.britannica.com/technology/solar-cell>
6. Khanna V.K. (2019). *Flexible Electronics, Volume 3 Energy devices and applications*. UK: IOP Publishing, Bristol.
7. Chakhmouradian, A. R., & Woodward, P. M. (2014). Celebrating 175 years of perovskite research: a tribute to Roger H. Mitchell. *Physics and Chemistry of Minerals*, 41(6), 387-391.
8. Goldschmidt, V. M. (1929). Crystal structure and chemical constitution. *Transactions of the Faraday Society*, 25, 253-283.
9. Bartel, C. J., Sutton, C., Goldsmith, B. R., Ouyang, R., Musgrave, C. B., Ghiringhelli, L. M., & Scheffler, M. (2019). New tolerance factor to predict the stability of perovskite oxides and halides. *Science advances*, 5(2), eaav0693.
10. Correa-Baena, J. P., Saliba, M., Buonassisi, T., Grätzel, M., Abate, A., Tress, W., & Hagfeldt, A. (2017). Promises and challenges of perovskite solar cells. *Science*, 358(6364), 739-744.

11. Nishiwaki, M., Narikuri, T., & Fujiwara, H. (2022). Crystal Structures. In Fujiwara H. Hybrid Perovskite Solar Cells: *Characteristics and Operation*. Weinheim, Germany Wiley-Vch. (67-89).
12. Basumatary, P., & Agarwal, P. (2022). A short review on progress in perovskite solar cells. *Materials Research Bulletin*, 149, 111700.
13. Rehman, W., McMeekin, D. P., Patel, J. B., Milot, R. L., Johnston, M. B., Snaith, H. J., & Herz, L. M. (2017). Photovoltaic mixed-cation lead mixed-halide perovskites: links between crystallinity, photo-stability and electronic properties. *Energy & Environmental Science*, 10(1), 361-369.
14. Li, C., Lu, X., Ding, W., Feng, L., Gao, Y., & Guo, Z. (2008). Formability of ABX₃ (X= F, Cl, Br, I) halide perovskites. *Acta Crystallographica Section B: Structural Science*, 64(6), 702-707.
15. Fujiwara, H. (2007). *Spectroscopic ellipsometry: principles and applications*. John Wiley & Sons.
16. Saliba, M., Matsui, T., Seo, J. Y., Domanski, K., Correa-Baena, J. P., Nazeeruddin, M. K., ... & Grätzel, M. (2016). Cesium-containing triple cation perovskite solar cells: improved stability, reproducibility and high efficiency. *Energy & environmental science*, 9(6), 1989-1997.
17. Fujiwara, H., & Wiley-Vch. (2022). *Hybrid perovskite solar cells: characteristics and operation*. Weinheim, Germany Wiley-Vch.)29-55.
18. Li, Z., Yang, M., Park, J. S., Wei, S. H., Berry, J. J., & Zhu, K. (2016). Stabilizing perovskite structures by tuning tolerance factor: formation of formamidinium and cesium lead iodide solid-state alloys. *Chemistry of Materials*, 28(1), 284-292.
19. Kato, M., Fujiseki, T., Miyadera, T., Sugita, T., Fujimoto, S., Tamakoshi, M., ... & Fujiwara, H. (2017). Universal rules for visible-light absorption in hybrid perovskite materials. *Journal of Applied Physics*, 121(11).
20. Jeon, N. J., Noh, J. H., Yang, W. S., Kim, Y. C., Ryu, S., Seo, J., & Seok, S. I. (2015). Compositional engineering of perovskite materials for high-performance solar cells. *Nature*, 517(7535), 476-480.
21. Anderson, B., & Anderson, R. (2004). *Fundamentals of semiconductor devices*. USA: McGraw-Hill, Inc.

22. Milot, R. L., Eperon, G. E., Snaith, H. J., Johnston, M. B., & Herz, L. M. (2015). Temperature-dependent charge-carrier dynamics in $\text{CH}_3\text{NH}_3\text{PbI}_3$ perovskite thin films. *Advanced Functional Materials*, 25(39), 6218-6227.
23. Smets, A., Jäger, K., Isabella, O., Van Swaaij, R., & Zeman, M. (2016). *Solar Energy: The physics and engineering of photovoltaic conversion, technologies and systems*. Bloomsbury Publishing.
24. Mitzi, D. B. (2000). Organic– inorganic perovskites containing trivalent metal halide layers: the templating influence of the organic cation layer. *Inorganic chemistry*, 39(26), 6107-6113.
25. Bi, Y., Hutter, E. M., Fang, Y., Dong, Q., Huang, J., & Savenije, T. J. (2016). Charge carrier lifetimes exceeding 15 μs in methylammonium lead iodide single crystals. *The journal of physical chemistry letters*, 7(5), 923-928
26. Perovskites, O. H. (2004). Efficient hybrid solar cells based on meso-superstructures. *Phys. Rev. Lett*, 92, 210403.
27. Tejada, A., Braunger, S., Korte, L., Albrecht, S., Rech, B., & Guerra, J. A. (2018). Optical characterization and bandgap engineering of flat and wrinkle-textured $\text{FA}0.83\text{Cs}0.17\text{Pb}(\text{I}1-\text{xBrx})_3$ perovskite thin films. *Journal of applied physics*, 123(17).
28. Edri, E., Kirmayer, S., Henning, A., Mukhopadhyay, S., Gartsman, K., Rosenwaks, Y., ... & Cahen, D. (2014). Why lead methylammonium tri-iodide perovskite-based solar cells require a mesoporous electron transporting scaffold (but not necessarily a hole conductor). *Nano letters*, 14(2), 1000-1004.
29. Löper, P., Stuckelberger, M., Niesen, B., Werner, J., Filipič, M., Moon, S. J., ... & Ballif, C. (2015). Complex refractive index spectra of $\text{CH}_3\text{NH}_3\text{PbI}_3$ perovskite thin films determined by spectroscopic ellipsometry and spectrophotometry. *The journal of physical chemistry letters*, 6(1), 66-71.
30. Leguy, A. M., Hu, Y., Campoy-Quiles, M., Alonso, M. I., Weber, O. J., Azarhoosh, P., ... & Barnes, P. R. (2015). Reversible hydration of $\text{CH}_3\text{NH}_3\text{PbI}_3$ in films, single crystals, and solar cells. *Chemistry of Materials*, 27(9), 3397-3407
31. Stoumpos, C. C., Malliakas, C. D., & Kanatzidis, M. G. (2013). Semiconducting tin and lead iodide perovskites with organic cations: phase transitions, high mobilities, and near infrared photoluminescent properties. *Inorganic chemistry*, 52(15), 9019-9038.

32. Ašmontas, S., & Mujahid, M. (2023). Recent progress in perovskite tandem solar cells. *Nanomaterials*, 13(12), 1886.
33. Weber, D. (1978). $\text{CH}_3\text{NH}_3\text{PbX}_3$, EIN PB (II)-system mit kubischer perowskitstruktur/ $\text{CH}_3\text{NH}_3\text{PbX}_3$, a Pb (II)-system with cubic perovskite structure. *Zeitschrift für Naturforschung B*, 33(12), 1443-1445.
34. Kawamura, Y., Mashiyama, H., & Hasebe, K. (2002). Structural study on cubic-tetragonal transition of $\text{CH}_3\text{NH}_3\text{PbI}_3$. *Journal of the Physical Society of Japan*, 71(7), 1694-1697.
35. Baikie, T., Fang, Y., Kadro, J. M., Schreyer, M., Wei, F., Mhaisalkar, S. G., ... & White, T. J. (2013). Synthesis and crystal chemistry of the hybrid perovskite $(\text{CH}_3\text{NH}_3)\text{PbI}_3$ for solid-state sensitised solar cell applications. *Journal of Materials Chemistry A*, 1(18), 5628-5641.
36. Poglitsch, A., & Weber, D. (1987). Dynamic disorder in methylammoniumtrihalogenoplumbates (II) observed by millimeter-wave spectroscopy. *The Journal of chemical physics*, 87(11), 6373-6378.
37. Jager K. & Albrecht S (2022). *Perovskite based tandem solar cells. Hybrid Perovskite Solar Cells- Characteristics and Operation* (463-500). Germany: Wiley WCH
38. Kato Y & Fujiwara H. (2022). *Numerical Values of Shockley-Queisser Limit. Hybrid Perovskite Solar Cells- Characteristics and Operation* (563-566). Germany: Wiley WCH.
39. Correa-Baena, J. P., Saliba, M., Buonassisi, T., Grätzel, M., Abate, A., Tress, W., & Hagfeldt, A. (2017). Promises and challenges of perovskite solar cells. *Science*, 358(6364), 739-744.
40. Bartel, C. J., Sutton, C., Goldsmith, B. R., Ouyang, R., Musgrave, C. B., Ghiringhelli, L. M., & Scheffler, M. (2019). New tolerance factor to predict the stability of perovskite oxides and halides. *Science advances*, 5(2), eaav0693.
41. Saliba, M., Matsui, T., Seo, J. Y., Domanski, K., Correa-Baena, J. P., Nazeeruddin, M. K., ... & Grätzel, M. (2016). Cesium-containing triple cation perovskite solar cells: improved stability, reproducibility and high efficiency. *Energy & environmental science*, 9(6), 1989-1997.

42. Li, Z., Yang, M., Park, J. S., Wei, S. H., Berry, J. J., & Zhu, K. (2016). Stabilizing perovskite structures by tuning tolerance factor: formation of formamidinium and cesium lead iodide solid-state alloys. *Chemistry of Materials*, 28(1), 284-292.
43. Shirayama, M., Kato, M., Miyadera, T., Sugita, T., Fujiseki, T., Hara, S., ... & Fujiwara, H. (2016). Degradation mechanism of CH₃NH₃PbI₃ perovskite materials upon exposure to humid air. *Journal of Applied Physics*, 119(11).
44. Yang, J., Siempelkamp, B. D., Liu, D., & Kelly, T. L. (2015). Investigation of CH₃NH₃PbI₃ degradation rates and mechanisms in controlled humidity environments using in situ techniques. *ACS nano*, 9(2), 1955-1963.
45. Philippe, B., Park, B. W., Lindblad, R., Oscarsson, J., Ahmadi, S., Johansson, E. M., & Rensmo, H. (2015). Chemical and Electronic Structure Characterization of Lead Halide Perovskites and Stability Behavior under Different Exposures□ A Photoelectron Spectroscopy Investigation. *Chemistry of Materials*, 27(5), 1720-1731.
46. Dong, X., Fang, X., Lv, M., Lin, B., Zhang, S., Ding, J., & Yuan, N. (2015). Improvement of the humidity stability of organic–inorganic perovskite solar cells using ultrathin Al₂O₃ layers prepared by atomic layer deposition. *Journal of Materials Chemistry A*, 3(10), 5360-5367.
47. Dada, T. M. (2021). *Fabrication and Characterization of Dye Sensitized Solar Cells using Locally Extracted Organic Dyes* (Doctoral dissertation, Obafemi Awolowo University).
48. Willoughby, A. A., Soge, A. A., Dairo, O. F., Olukanni, O. D., Durugbo, E. U., Michael, W. S., & Adebayo, T. A. (2021). Fabrication and Characterization of a Dye-Sensitized Solar Cell using Natural Dye Extract of Rosella (*Hibiscus sabdariffa* L.) as Photosensitizer. *Journal of the Nigerian Society of Physical Sciences*, 287-291.
49. Li, Y., Ji, L., Liu, R., Zhang, C., Mak, C. H., Zou, X., ... & Hsu, H. Y. (2018). A review on morphology engineering for highly efficient and stable hybrid perovskite solar cells. *Journal of Materials Chemistry A*, 6(27), 12842-12875.
50. Jager K. & Albrecht S (2022). *Perovskite based tandem solar cells. Hybrid Perovskite Solar Cells- Characteristics and Operation* (463-500). Germany: Wiley WCH.
51. Filip, M. R., Eperon, G. E., Snaith, H. J., & Giustino, F. (2014). Steric engineering of metal-halide perovskites with tunable optical band gaps. *Nature communications*, 5(1), 5757.

52. Dong, Q., Fang, Y., Shao, Y., Mulligan, P., Qiu, J., Cao, L., & Huang, J. (2015). Electron-hole diffusion lengths $> 175 \mu\text{m}$ in solution-grown $\text{CH}_3\text{NH}_3\text{PbI}_3$ single crystals. *Science*, 347(6225), 967-970.
53. Engr Fahad. (Year). *Different Types of Junction Methods in Electronics*. Electronic Clinic; Electronic Clinic. https://www.electronicclinic.com/different-types-of-junction-methods-in-electronics/#Grown_Junction_Method
54. Momblona, C., Malinkiewicz, O., Roldán-Carmona, C., Soriano, A., Gil-Escrig, L., Bandiello, E., ... & Bolink, H. J. (2014). Efficient methylammonium lead iodide perovskite solar cells with active layers from 300 to 900 nm. *Apl Materials*, 2(8).
55. Ponti, C., Nasti, G., Di Girolamo, D., Cantone, I., Alharthi, F. A., & Abate, A. (2022). Environmental lead exposure from halide perovskites in solar cells. *Trends in Ecology & Evolution*, 37(4), 281-283.
56. Afghan, S. A., Almusawi, H., & Geza, H. (2017). Simulating the electrical characteristics of a photovoltaic cell based on a single-diode equivalent circuit model. In *MATEC Web of Conferences* (Vol. 126, p. 03002). EDP Sciences.
57. Pandey, A., Pandey, P., & Tumuluru, J. S. (2022). Solar Energy Production in India and Commonly Used Technologies—An Overview. *Energies* 2022, 15, 500.
58. Dawson, M., Ribeiro, C., & Morelli, M. R. (2022). A review of three-dimensional tin halide perovskites as solar cell materials. *Materials research*, 25, e20210441.

Glossary

Junction- Meeting of two points or regions that creates an interface with each other

Diffusion- The physical or the biological process of spreading out or dispersing of the particles from the larger concentration (ratio) to the lower one.

Biasing- Electrical diode arrangement that allows uni-directional flow of the current after applying the external voltage.

Solar Cell- The electrical device that transforms the photo-energy (i.e. light energy) into heat energy.

Photovoltaics (PV)- The process of transforming the heat energy of the solar cell into the electrical form/ thermal energy with the help of semiconducting materials.

Perovskites- Material consisting of ABX_3 structure that is similar to that of minerals like calcium titanium oxide.

Hybrid Perovskites- It can be described as a semiconducting material of ABX_3 type that consists of organic as well as inorganic molecules like alkyls, aromatic ions, oxides and halides.

Homo junction- Semiconductor interface/layer created between the two identical material types. Homo- means “Single/One”.

Heterojunction- Multiple layers/interfaces created between the two semiconducting materials but of different types. Hetero- means “Two or more/Multiple”.

Mesoscopic- The size of materials lying between the range of nano meters (nm) to few micrometers (μm).

Tandem- Two or more groups/cells arranged one behind/below the other that can be used to generate power output in terms of voltage or current.

Sustainability- A continuous effort/ initiative to support and sustain the process/methods that are economically, socially and environmentally safe/reproducible for all. Example: Tree-plantation programme, Bio energy fuels, Electric vehicles, etc.